

Supporting Information for

Uncorrelated Dynamical Processes in Tetranuclear Carboxylate Clusters Studied by Variable Temperature ^1H NMR Spectroscopy

Femke F. B. J. Janssen, Laurens C. J. M. Peters, Paul P. J. Schlebos, Jan M. M. Smits, René de
Gelder, Alan E. Rowan*

*Radboud University Nijmegen, Institute for Molecules and Materials, Heyendaalseweg 135, 6525
AJ Nijmegen, The Netherlands*

Experimental Procedures	S3
Figure 1. Powder Diffraction Patterns of 1b and 1c .	S7
Crystallographic Data.	S8
Thermal Ellipsoid Plots.	S10
Figure 2: ORTEP of 1a .	S10
Figure 3: ORTEP of 1c .	S10
Figure 4: ORTEP of 2a .	S11
Figure 5. ORTEP of 3 .	S11
Figure 6. ORTEP of 4 .	S12
Figure 7. ORTEP of 5 .	S12
Figure 8. ¹³ C NMR Spectrum of 1a .	S14
Variable Temperature NMR Spectroscopy	S15
Figure 9: Variable temperature NMR spectra of 1a	S17
Figure 10: Variable temperature NMR spectra of 2a	S18
Figure 11: Variable temperature NMR spectra of 1b	S19
Figure 12: Variable temperature NMR spectra of 2b	S20
Figure 13: Eyring plot of dynamics for 1a	S21
Figure 14: Eyring plot of dynamics for 2a	S21
References	S22

Experimental Procedures

Instrumentation ^1H NMR, $^{13}\text{C}\{^1\text{H}\}$ NMR, COSY and 2D NOESY spectra were recorded on a Bruker Advance 500 MHz operating at room temperature or on a Bruker DPX-200 MHz. Chemical shifts are reported in ppm using the deuterated solvent peaks as a reference. Abbreviations used are: s = singlet, t = triplet, dd = doublet of doublets, ddd = doublet of doublet of doublets, dt = double triplet, m = multiplet, br. = broad. The assignment of the peaks is given in the main text of this article. Coupling constants are reported as J-values in Hz. X-ray powder diffraction measurements were performed either on a Bruker D8 AXS Advance X-ray diffractometer equipped with a Vântec-1 detector or on a Philips PW 1820 Automatic Powder Diffractometer. The patterns were measured in reflection mode with Bragg-Brentano geometry using monochromatic $\text{CuK}\alpha$ radiation in the range from 2 to $50^\circ 2\theta$. The scan speed and step size depended on the quality of the sample. Powder patterns were simulated with $\text{Cu K}\alpha_1$ radiation in the range of 2 to $50^\circ 2\theta$ with a step size of 0.02. Elemental analysis was performed on a Carlo Erba Instruments CHNS-O EA1108 Elemental analyzer or were carried out by the Analytische Laboratorien in Lindlar (Germany).

Materials 2,6-diformylpyridine was prepared according to literature procedures.¹ 4-chloro-2,6-diacetylpyridine was obtained from HetCat. All other materials were obtained commercially and used without any further purification.

$[\text{Cd}(\text{O}_2\text{CC}_6\text{H}_5)_2] \cdot 4/3\text{H}_2\text{O}$ To a solution of $3\text{CdSO}_4 \cdot 8\text{H}_2\text{O}$ (5.0 g, 6.5 mmol) in H_2O (20 ml) was added sodium benzoate (5.6 g, 39 mmol) dissolved in a minimal amount of water. The formed precipitate was isolated by filtration and dried in air. Yield 4.9 g (66%). The product was identified as $[\text{Cd}(\text{O}_2\text{CC}_6\text{H}_5)_2] \cdot 3/4\text{H}_2\text{O}$ by elemental analysis. Elemental analysis calculated (%) for $\text{CdC}_{14}\text{H}_{38/3}\text{O}_{16/3}$: C 44.41, H 3.37, O 22.54; found: C 44.23, H 3.54, O 22.70.

$[\text{Zn}(\text{O}_2\text{CC}_6\text{H}_5)_2] \cdot 3/8\text{H}_2\text{O}$ To a solution of sodium benzoate (10.6 g, 73.4 mmol) in H_2O (75 ml) at 80°C was added a solution of ZnCl_2 (5.0 g, 36.7 mmol) in H_2O (20 ml). Immediately a precipitate was formed. The mixture was stirred at 80°C for 10 min before allowing it to cool to room temperature. The white solid was isolated by filtration and dried in air. The product was identified as $[\text{Zn}(\text{O}_2\text{CC}_6\text{H}_5)_2] \cdot 3/8\text{H}_2\text{O}$. The IR spectrum corresponded with literature.^{2,3} Elemental analysis calculated (%) for $\text{ZnC}_{14}\text{H}_{86/8}\text{O}_{35/8}$: C 53.49 H 3.45; found: C 53.44, H 3.16.

[Zn₄(L)₂(O₂CCH₃)₄] · 3MeOH (1a) A solution of 2-aminophenol (2.0 g, 18.3 mmol), 2,6-diacetylpyridine (1.5 g, 9.2 mmol) and zinc acetate dihydrate (4.02 g, 18.3 mmol) in methanol (40 ml) was refluxed for 3 h. After cooling down, the solvent was removed. To the residue was added toluene (20 ml) and the solvent was removed again (toluene-acetic acid azeotrope). The addition and removal of toluene was repeated until the residue was no longer sticky. The dry residue was dissolved in methanol (15 ml) and the cluster was precipitated with Et₂O (30 ml). After stirring for 20 min the yellow precipitate was isolated by filtration. Yield 5.0 g (92.8%). Single crystals were obtained from a methanol solution top-layered with Et₂O. The assignment of the peaks at low and high temperature was achieved using a COSY and 2D NOESY spectrum. ¹H NMR (500 MHz, DMF-*d*₇, 357 K): δ = 1.25 (s, 12H), 2.82 (s, 12H), 6.56 (t, 4H, ³*J* = 7.5 Hz), 6.88 (t, 4H, ³*J* = 7.5 Hz), 7.06 (d, 4H, ³*J* = 7.5 Hz), 7.27 (d, 4H, ³*J* = 7.5 Hz), 8.08 (d, 4H, ³*J* = 7.5 Hz), 8.20 (d, 2H, ³*J* = 7.5 Hz). ¹H NMR (500 MHz, DMF-*d*₇, 257 K): δ = 0.80 (s, 6H), 1.33 (s, 6H), 2.74 (s, 6H), 2.96 (s, 6H), 6.41 (t, 2H, ³*J* = 7.5 Hz), 6.62 (t, 2H, ³*J* = 7.5 Hz), 6.76 (t, 2H, ³*J* = 7.5 Hz), 6.89 (d, 2H, ³*J* = 7.5 Hz), 6.96 (d, 2H, ³*J* = 7.5 Hz), 7.06 (t, 2H, ³*J* = 7.5 Hz), 7.11 (d, 2H, ³*J* = 7.5 Hz), 7.60 (d, 2H, ³*J* = 7.5 Hz), 8.11 (d, 2H, ³*J* = 7.5 Hz), 8.20 (d, 2H, ³*J* = 7.5 Hz), 8.25 (t, 2H, ³*J* = 7.5 Hz). ¹³C NMR (125 MHz, DMF-*d*₇, 242 K): δ = 16.4, 18.1, 20.0, 22.9, 117 (2C), 120.2, 121.7, 123.5, 123.6, 124.2, 124.5, 128.0, 129.4, 134.7, 136.3, 143.2, 148.7, 150.8, 156.7, 158.0, 158.4, 160.0, 176.3, 179.5. Elemental analysis calculated (%) for C₅₃H₅₈N₆O₁₅Zn₄: C 49.71, H 4.56, N 6.56; found: C 49.12, H 4.63, N 6.57.

[Cd₄(L)₂(O₂CCH₃)₄] · DMF · H₂O (2a) The compound is synthesized according to a modified literature procedure.⁴ A solution of 2-aminophenol (2.0 g, 18.3 mmol), 2,6-diacetylpyridine (1.5 g, 9.2 mmol) and Cd(O₂CCH₃)₂ · 2H₂O (4.9 g, 18.4 mmol) in DMF (50 ml) was refluxed for 3 h. During cooling to room temperature an orange/red precipitate was formed, which was isolated by filtration. Single crystals were obtained from a DMF solution top-layered with Et₂O. Yield 3.4 g (51 %). ¹H NMR (500 MHz, DMF-*d*₇, 257 K): δ = 0.98 (s, 6H), 1.43 (s, 6H), 2.75 (s, 6H), 3.03 (s, 6H), 6.37 (dt, 2H, ³*J* = 7.5 Hz, ⁴*J* = 1.5 Hz), 6.53 (dd, 2H, ³*J* = 7.5 Hz, ⁴*J* = 1.5 Hz), 6.63 (dt, 2H, ³*J* = 7.5 Hz, ⁴*J* = 1.5 Hz), 6.81 (dt, 2H, ³*J* = 7.5 Hz, ⁴*J* = 1.5 Hz), 7.02 (dd, 2H, ³*J* = 7.5 Hz, ⁴*J* = 1.5 Hz), 7.16 (m, 6H, overlapping signals), 8.18 (dd, 2H, ³*J* = 5.5 Hz, ⁴*J* = 3.0 Hz), 8.32 (m, 4H, overlapping signals). High temperature NMR (357 K) gave only very broad peaks and these were difficult to assign. The bulk of the crystals was identified via powder diffraction to be **2a**.

[Zn₄(L)₂(O₂CCH₃)(O₂CC₆H₅)₃] (1c) To a solution of **1a** (300 mg, 0.23 mmol) in MeOH (20 ml) was added benzoic acid (5 eq., 143 mg, 1.17 mmol) dissolved in a minimal amount of MeOH under vigorous stirring. After a few minutes the solution became turbid. Upon stirring for 30 min a yellow precipitate was isolated by filtration. Powder diffraction of this crude material showed that it contained the exchanged product. The yield was not determined. Single crystals could be grown from a similar reaction procedure, but without stirring. To a solution of **1a** (100 mg, 80 μmol) in MeOH (10 ml) was added benzoic acid (50 mg, 0.41 mmol) dissolved in a minimal amount of MeOH. After 24h single-crystals could be isolated. But, unfortunately, a satisfactory elemental analysis could not be obtained.

[Zn₄(L)₂(O₂CC₆H₅)₄] (1b) To a solution of [Zn(O₂CC₆H₅)₂] · 3/8H₂O (2.0 g, 6.4 mmol) in MeOH (100 ml) at 70°C was added a solution of 2,6-diacetylpyridine (530 mg, 3.25 mmol) and 2-aminophenol (696 mg, 6.4 mmol) in MeOH (40 ml). This solution was refluxed for 3 h during which a yellow precipitate was formed. After cooling to room temperature the precipitate was isolated by filtration. Yield 1.38 g (55%). The ¹H NMR is rather complicated and an assignment of the peaks is given in the main text of this article. Although the material stays crystalline over time, powder diffraction showed a change in pattern, indicating solvent loss. The crystal structure determination on **1c** suggested the presence of MeOH and H₂O in the crystal lattice. The elemental analysis gave a satisfactory match for a compound with the composition [Zn₄(L1)₂(O₂CC₆H₅)₄] · 3MeOH · 2H₂O. Elemental analysis calculated (%) for C₇₃H₇₀N₆O₁₇Zn₄: C 56.03, H 4.51, N 5.37; found: C 56.14, H 4.46, N 5.50.

[Cd₄(L)₂(O₂CC₆H₅)₄] (2b) A solution of 2,6-diacetylpyridine (250 mg, 1.53 mmol), 2-aminophenol (334 mg, 3.1 mmol) and [Cd(O₂CC₆H₅)₂] · 4/3H₂O (1.0 g, 2.6 mmol) was refluxed in MeOH (10 ml) for 3 h. After cooling to room temperature the precipitate was isolated by filtration. Yield 0.41 g (61%). The ¹H NMR at 348 K still showed some broadening of the signals and assignment of the peaks is therefore not reported. The assignment of the peaks at low temperature was achieved using a COSY spectrum. ¹H NMR (500 MHz, DMF-*d*₇, 248 K): δ = 2.75 (s, 6H), 3.19 (s, 6H), 6.20 (t, 2H, ³J = 7.5 Hz), 6.25 (t, 2H, ³J = 7.5 Hz), 6.61 (t, 2H, ³J = 7.5 Hz), 6.74 (t, 2H, ³J = 7.5 Hz), 6.78 (d, 2H, ³J = 7.5 Hz), 6.94 (d, 2H, ³J = 7.5 Hz), 6.96 (d, 2H, ³J = 7.5 Hz), 6.98 (d, 4H, ³J = 7.5 Hz), 7.15 (t, 2H, ³J = 7.5 Hz), 7.26 (d, 4H, ³J = 7.5 Hz), 7.34 (d, 2H, ³J = 7.5 Hz), 7.42 (t, 4H, ³J = 7.5 Hz), 7.50 (t, 2H, ³J = 7.5 Hz), 7.91 (d, 4H, ³J = 7.5 Hz), 8.26 (d, 2H, ³J = 7.5 Hz), 8.39 (d, 2H, ³J = 7.5

Hz), 8.42 (t, 2H, $^3J = 7.5$ Hz). The crystal structure determination on **1c** suggested the presence of MeOH and H₂O in the crystal lattice. The elemental analysis gave a satisfactory match for a compound with the composition [Cd₄(L)₂(O₂CC₆H₅)₄] · MeOH · 6H₂O. Elemental analysis calculated (%) for C₇₁H₇₀Cd₄N₆O₁₉: C 48.43, H 4.01, N 4.77, Cd 25.53; found: C 48.24, H 3.90, N 4.83, Cd 25.82.

Zn₄(L2)₂(O₂CCH₃)₄ · 2CHCl₃ · 2H₂O (3) To a solution of 878 mg zinc acetate dihydrate (4.0 mmol), 250 mg 2,6-diformylpyridine (2.0 mmol) and 660 mg 2-amino-4-*tert*-butylphenol (4.0 mmol) in 20 ml methanol was refluxed for 1 hour. After cooling to r.t. the solvent was removed. The residue was dissolved in toluene to remove the excess acetic acid via azeotropic evaporation. This was repeated twice to yield a dark red solid. Single-crystals were grown from a chloroform solution top-layered with diethylether. During the preparation of the sample for elemental analysis some chloroform solvent was evaporated from the sample, because a good elemental analysis could be found for a compound with the composition Zn₄(L2)₂(O₂CCH₃)₄ · CHCl₃ · 2H₂O. Elemental analysis calculated for Zn₄C₆₃H₇₁N₆O₁₄Cl₃: C 50.31, H 4.76, N 5.59. Found: C 50.31, H 5.03, N 5.71.

Zn₂(L3)(O₂CCH₃)₂(DMF) · 2DMF (4) A solution of 439 mg zinc acetate dihydrate (2.0 mmol), 135 mg 2,6-diformylpyridine (1.0 mmol) and 220 mg 2-aminophenol (2.0 mmol) in 10 ml methanol was refluxed for 1 hour. After cooling to r.t. the orange precipitate of unknown composition was isolated by filtration. This orange precipitate was dissolved in boiling DMF. After cooling to r.t. the product was precipitated with a large amount of diethylether. Single-crystals could be grown from a DMF solution top-layered with diethylether. The product was not further analyzed.

[Zn₄(L4)₂(O₂CCH₃)₄] (5) A solution of 80 mg 4-chloro-2,6-diacetylpyridine (0.4 mmol), 80 mg 2-aminophenol (0.4 mmol) and 175.6 mg zinc acetate dihydrate (0.8 mmol) in 60 ml methanol was refluxed for 3 hours. The solution was cooled to r.t. and the solvent was evaporated. The crude was dissolved in a minimal amount of methanol and precipitated with diethylether. Single crystals could be grown from a methanol solution top-layered with diethylether. ¹H NMR (500 MHz, DMF-*d*₇, 253 K): δ = 0.83 (s, 6H), 1.34 (s, 6H), 2.81 (s, 6H), 2.98 (s, 6H), 6.51 (t, 2H, $^3J = 7.5$ Hz), 6.73 (t, 2H, $^3J = 7.5$ Hz), 6.78 (t, 2H, $^3J = 7.5$ Hz), 6.89 (d, 2H, $^3J = 7.5$ Hz), 7.04 (d, 2H, $^3J = 7.5$ Hz), 7.09 (t, 2H, $^3J = 7.5$ Hz), 7.15 (d, 2H, $^3J = 7.5$ Hz), 7.59 (d, 2H, $^3J = 7.5$ Hz), 8.32 (d, 2H, $^4J = 1.5$ Hz), 8.44 (d, 2H, $^4J = 1.5$ Hz).

Powder Diffraction Patterns of **1b** and **1c**.

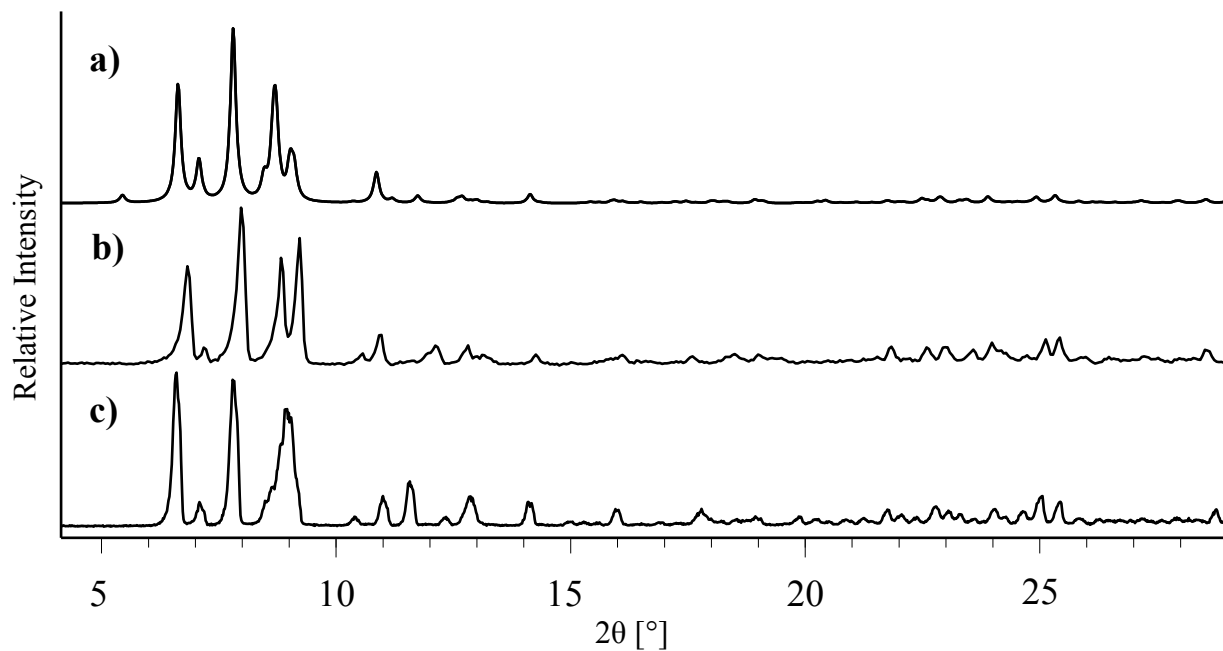


Figure 1. Comparison between a) simulated powder pattern of $[\text{Zn}_4(\text{L})_2(\text{O}_2\text{CCH}_3)(\text{O}_2\text{CC}_6\text{H}_5)_3]$ (**1c**). b) Experimental powder pattern of $[\text{Zn}_4(\text{L})_2(\text{O}_2\text{CCH}_3)(\text{O}_2\text{CC}_6\text{H}_5)_3]$ (**1c**). c) Experimental powder pattern of $[\text{Zn}_4(\text{L})_2(\text{O}_2\text{CC}_6\text{H}_5)_4]$ (**1b**).

Crystallographic Data.

Single crystal diffraction was performed on a Nonius KappaCCD single-crystal diffractometer (φ and ω scan mode) using graphite monochromated MoK α radiation. Intensity data were corrected for Lorentz and polarization effects. A semi-empirical multiscan absorption correction was applied (SADABS).⁵ The structures were solved with the Patterson search methods (DIRDIF).⁶ The structures were refined with the standard methods (refinement against F^2 of all reflections with SHELXL97)⁷ with anisotropic displacement parameters for the non-hydrogen atoms. The hydrogen atoms were placed at calculated positions and refined riding on the parent atoms unless indicated otherwise.

At the end of the anisotropic least-squares refinement of compound **1a** there were some residual electron densities present, which could not be modeled satisfactorily using disordered and partially occupied solvent molecules. Bond distances and thermal displacement parameters were physically unacceptable. Therefore the SQUEEZE procedure of PLATON (Spek, 2003) was applied to account for these electron densities. The analysis showed two voids of 222 Å³ containing 53 electrons each. We assume that each void contains two disordered methanol moieties, and the physical data reported here are based on that assumption. During the refinement of **1c** it became clear that only two of the four benzoate ligands are fully occupied and that the other two are partly replaced by acetate ligands in a mean ratio of about 2:1. The site occupancy factors of the C₆H₅ moieties of the benzoate ligands, and hence of the CH₃ moieties of the acetate ligands, were refined separately. The OOC moieties of both types of ligands were given unit site occupancy factors because of too large correlation factors when refined separately. And although the C₆H₅ moieties were constrained to have the same geometry as the fully occupied benzoate ligands, bond distances and angles are not very reliable. At the end the anisotropic refinement, including one methanol and a single oxygen atoms on which no hydrogen atoms could be located, still showed a number of rather high residual density peaks. Attempts to assign partially occupied, disordered methanol molecules to these peaks invariably resulted in physically unacceptable bond distances and thermal displacement parameters. It should be noted that no too short intermolecular distances were detected. Eventually the SQUEEZE procedure of PLATON (Spek, 2003) was used to account for these residual densities. However, this showed 4 voids of a mere 18 Å³ containing 7 electrons and 4 voids of 96 Å³, containing 22 electrons. As a consequence the influence of the SQUEEZE procedure is rather limited. Nevertheless, it is not unlikely that some additional solvent molecules are present in the

structure in place of the missing benzoate ligands, although some volumes of the detected voids are not sufficient to accommodate additional solvent molecules. We assume that the SQUEEZE procedure cannot detect voids that result from partially occupied ligands. It is virtually impossible to give the exact chemical composition of the compound. The physical data given in Table S1 are based on the assumption that all benzoate are fully occupied, partly to compensate for the missing solvent molecules. This means that the number of carbon atoms in the whole unit cell is somewhere between 272 and 284, and the number of hydrogen atoms between 228 and 232. A few atoms in the other ligands show rather large anisotropic thermal displacement parameters. It proved impossible to refine a disordered model for these atoms. Attempts to do so resulted in unstable refinements. Moreover, two disordered atoms, C44B and C65B, had to be refined isotropically to keep the displacement parameters physically acceptable. At the end the anisotropic least-squares refinement of compound **4** showed some residual electron densities which could not be modeled satisfactorily using disordered and partially occupied solvent molecules. Bond distances and thermal displacement parameters were physically unacceptable. Therefore, the SQUEEZE procedure of PLATON (Spek, 2003) was applied to account for these electron densities. The analysis showed two voids of 529 Å³ containing 176 electron each. We assume that each void contains four disordered DMF moieties, and the physical data reported here are based on that assumption. At the end of the anisotropic least-squares refinement of compound **5** there were some residual electron densities present, which could not be modeled satisfactorily using disordered and partially occupied solvent molecules. Bond distances and thermal displacement parameters were physically unacceptable. Therefore the SQUEEZE procedure of PLATON (Spek, 2003) was applied to account for these electron densities. The analysis showed four voids of 79 Å³ containing 21 electrons each. We assume that each void contains one disordered diethylether moieties, and the physical data reported here are based on that assumption.

THERMAL ELLIPSOID PLOTS.

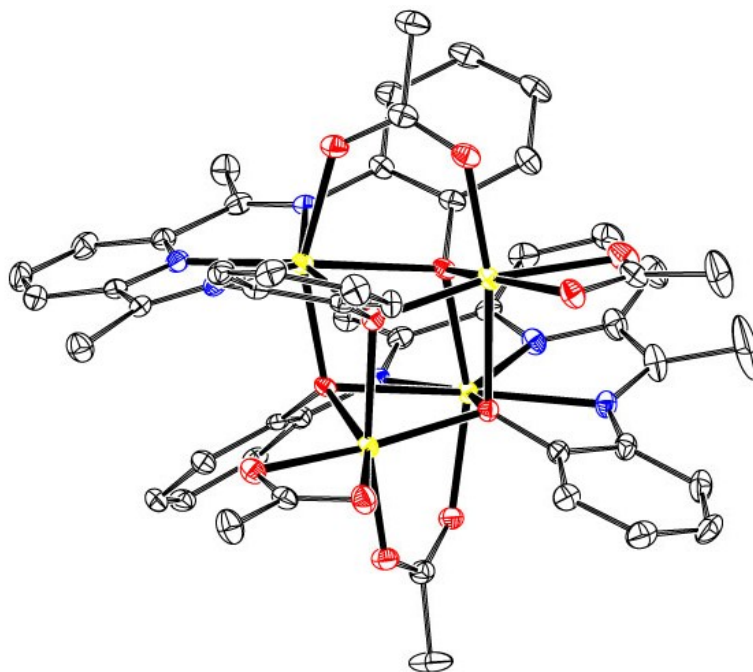


Figure 2. Thermal ellipsoids plot drawn at a probability level of 50% of the crystal structure (98K) of $[\text{Zn}_4(\text{L})_2(\text{O}_2\text{CCH}_3)_4]$ (**1a**).

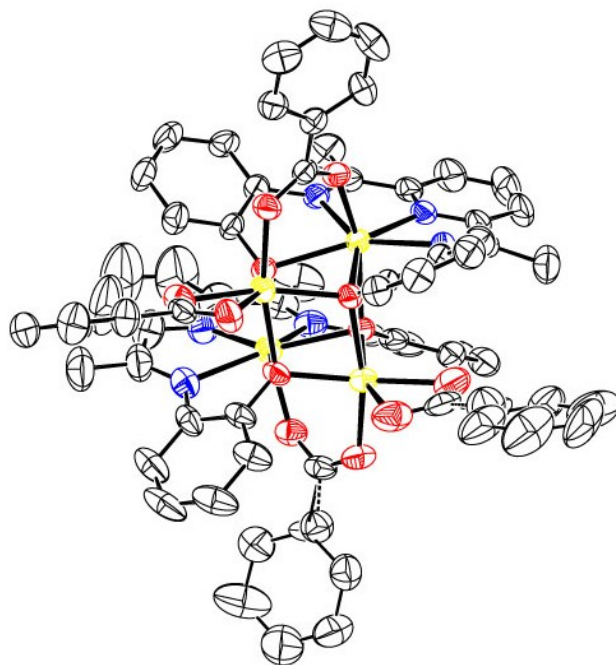


Figure 3. Thermal ellipsoids plot drawn at a probability level of 50% of the crystal structure of $[\text{Zn}_4(\text{L})_2(\text{O}_2\text{CCH}_3)(\text{O}_2\text{CC}_6\text{H}_5)_3]$ (**1c**).

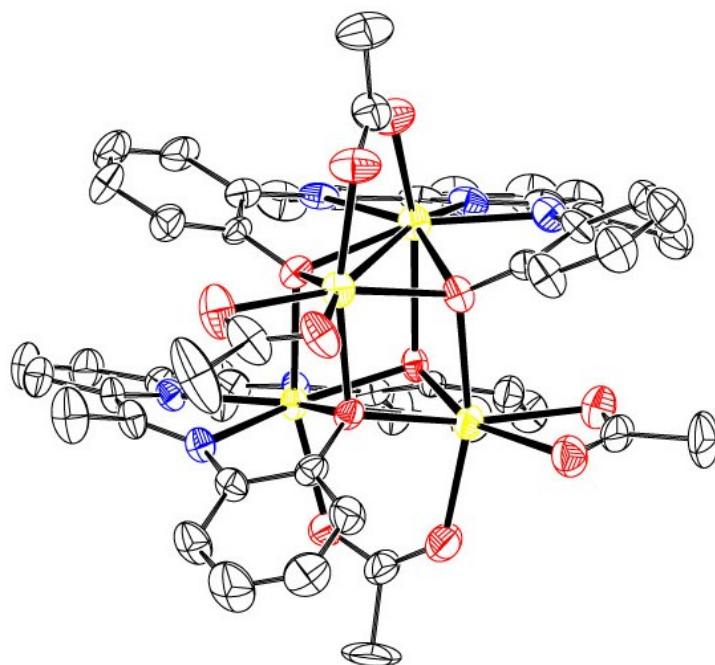


Figure 4. Thermal ellipsoids plot drawn at a probability level of 50% of the crystal structure of [Cd₄(L)₂(O₂CCH₃)₄] (2a).

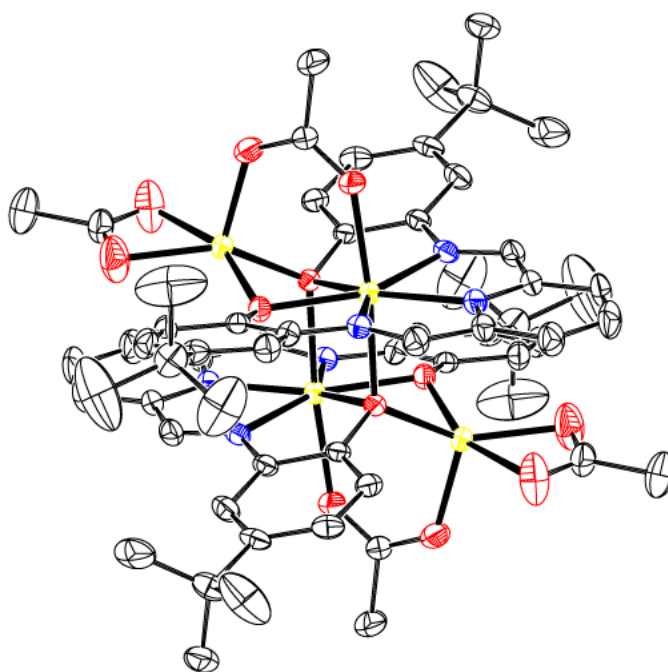


Figure 5. Thermal ellipsoids plot drawn at a probability level of 50% of the crystal structure of [Zn₄(L₂)₂(O₂CCH₃)₄] (3).

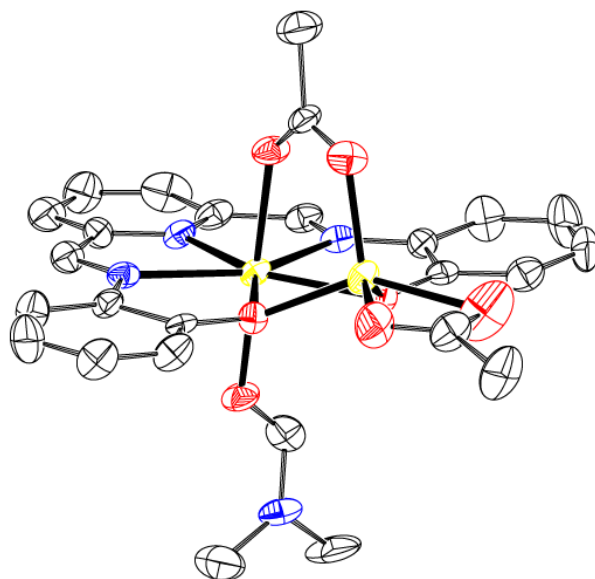


Figure 6. Thermal ellipsoids plot drawn at a probability level of 50% of the crystal structure of $\text{Zn}_2(\text{L}2)(\text{O}_2\text{CCH}_3)_2(\text{DMF}) \cdot 2\text{DMF}$ (**4**).

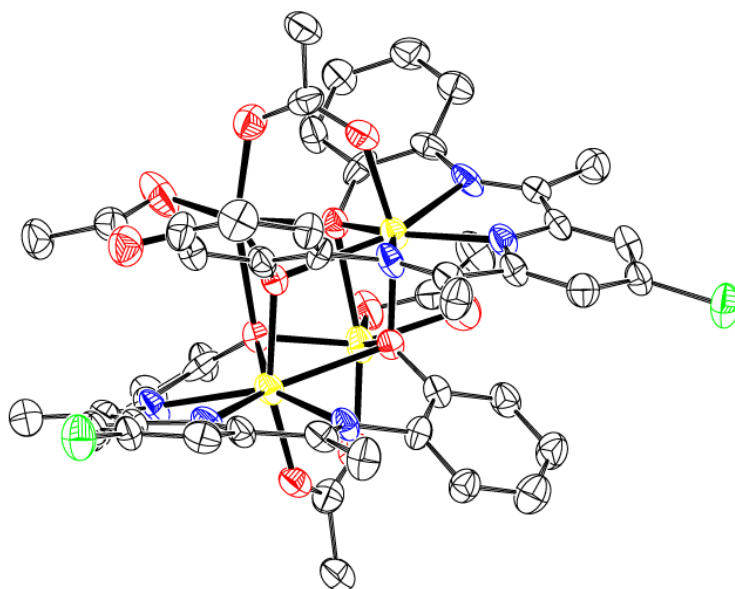


Figure 7. Thermal ellipsoids plot drawn at a probability level of 50% of the crystal structure of $[\text{Zn}_4(\text{L}3)_2(\text{O}_2\text{CCH}_3)_4]$ (**5**).

^{13}C NMR SPECTRUM OF $\text{Zn}_4(\text{L})_2(\text{O}_2\text{CCH}_3)_4$ (1a**).**

In Figure 8 the $^{13}\text{C}\{^1\text{H}\}$ NMR spectrum of **1a** measured at 257 K is shown. The assignment of the carbon atoms 1, 2, 5 and 7-10 was achieved via 2D CH-CORR spectrum. The two signals at 179.8 and 176.5 ppm are assigned to the carbonyl signals of the acetate groups. Solution and solid state $^{13}\text{C}\{^1\text{H}\}$ NMR studies on Zn and Zr carboxylate clusters have shown that the C=O resonance of chelating carboxylate ligands lie more downfield than C=O resonances of other types of carboxylate coordination modes.⁸ The exact chemical shift of the C=O resonance of the different coordination modes of the carboxylate ligand is variable and depends on the coordination mode of the metal atom as well as the type of metal.^{8d,9} We have, therefore, tentatively assigned the peak at 179.8 ppm to the C=O of the chelating and the peak at 176.5 ppm to the C=O of the bridging carboxylate. The COLOC spectrum showed a long range correlation between the $^{13}\text{C}\{^1\text{H}\}$ carbon resonance at 179.8 ppm and the ^1H proton resonance at 1.33 ppm, which led to the assignment of the proton resonance at 1.33 ppm to the chelating carboxylate ligand. In combination with a CH-CORR spectrum the peak at 20.3 ppm in the carbon spectrum is assigned to the CH_3 resonance of the acetate ligand. The assignment of the carbon atoms 3, 4, 6 and 11 are based on the spectra of other diiminepyridine ligands, but remains tentative.¹⁰

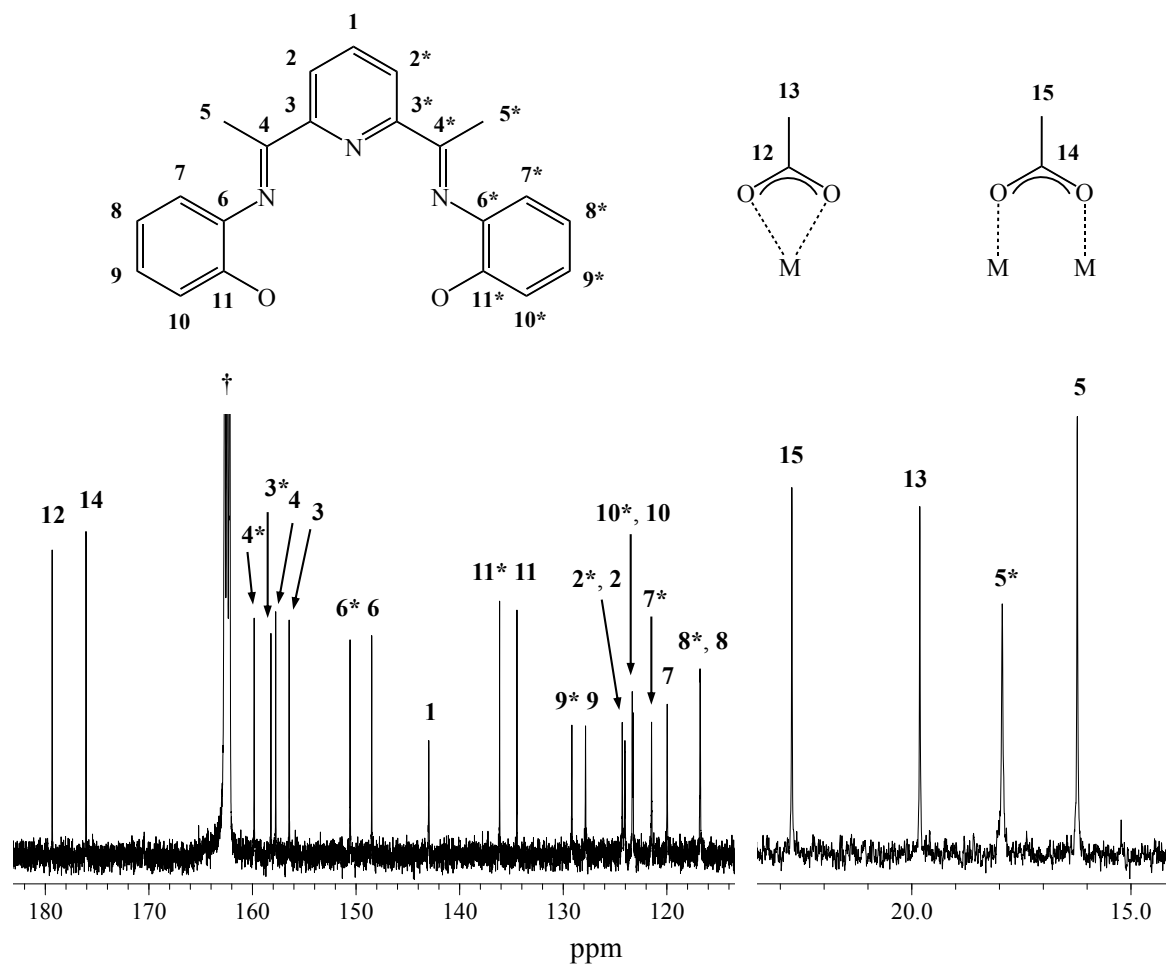


Figure 8. ¹³C NMR spectrum of Zn₄(L)₂(O₂CCH₃)₄ (**1a**) in DMF-*d*₇ measured at 250 K. The * indicates that the corresponding carbon atom is shielded by the aromatic system of the other ligand in the cluster. † = DMF-*d*₇ solvent peaks. The assignment of carbon atoms 3, 4, 6 and 11 is tentative.

VARIABLE TEMPERATURE NMR SPECTROSCOPY: The VT-NMR experiments were performed on a Bruker Advance 500 operating at 500 MHz and 125 MHz in the temperature range 242 K to 357 K with steps of 5 K. The temperature calibrated using 100% ethylene glycol and 100% methanol.¹¹ VT-NMR provides the possibility for determination of the kinetic parameters of the dynamic process. The most accurate rate constants are obtained by using a full line-shape analysis, but our spectra suffer from significant overlap between the peaks hampering a good comparison with calculated line shapes. However, good estimates of these values can be obtained by using well established approximations. In the “coalescence method” the rate constant at different temperatures is estimated using the difference in chemical shifts of the exchanging proton.^{12,13} This approximation is valid when the sites of exchange are equally populated and $(\nu_A - \nu_B)$ is large compared with half-height line-widths ω_{a0} and ω_{b0} .¹⁴ In our tetranuclear clusters the two site exchange model is perhaps not completely applicable, but nevertheless the activation parameters deduced from this approximation will give an indication about the possible dynamical mechanisms.

The rate constant at the coalescence point is determined by using Equation 1,

$$k_{T_c} = \frac{\pi \Delta \nu_0}{\sqrt{2}} \quad (1)$$

where k_{T_c} is the rate constant at the coalescence point, and $\Delta \nu_0$ is the maximum chemical shift difference (in Hz) for a particular proton in the absence of exchange. The Eyring equation (Equation 2) can be rearranged into Equation 3, which allows the estimation of the Gibbs energy of activation (ΔG^\ddagger) at the coalescence temperature,

$$k_{T_c} = \frac{k_b \times T_c}{h} e^{\frac{-\Delta G^\ddagger}{RT_c}} \quad (2)$$

where R is the gas constant, T_c is the coalescence temperature, k_{T_c} is the rate constant at coalescence, h is Planck's constant, k_b is Boltzmann's constant.

$$\Delta G^\ddagger = -RT_c \ln \left(\frac{k_{T_c} \times h}{k_b \times T_c} \right) \quad (3)$$

For temperatures below and up to the coalescence point the rate constants are determined by using Equation 4,

$$k_{T < T_c} = \frac{\pi}{\sqrt{2}} (\Delta\nu_0^2 - \Delta\nu_e^2)^{\frac{1}{2}} \quad (4)$$

where $k_{T < T_c}$ is the rate constant for temperatures below the coalescence point, $\Delta\nu_0$ is the maximum chemical shift difference (in Hz) for a particular exchanging proton, $\Delta\nu_e$ is the chemical shift difference (in Hz) for a proton at a particular temperature.

These rate constants can be used to construct an Eyring plot ($\ln(k/T)$ vs $1/T$) by substituting Equation 5 into Equation 2 and rearranging it to Equation 6. The intercept and the slope of this plot lead to estimated values of ΔH^\ddagger and ΔS^\ddagger (respectively, enthalpy and entropy of activation).

$$\Delta G^\ddagger = \Delta H^\ddagger - T\Delta S^\ddagger \quad (5)$$

$$\ln\left(\frac{k}{T}\right) = \frac{-\Delta H^\ddagger}{R}\left(\frac{1}{T}\right) + \left(\ln\frac{k_b}{h} + \frac{\Delta S^\ddagger}{R}\right) \quad (6)$$

The error in ΔG^\ddagger has been estimated to be larger than 10%, but it has been shown that this value is not very sensitive to large errors in temperature or rate constant.¹⁵ The error in ΔH^\ddagger and ΔS^\ddagger are the standard deviations obtained by linear regression analysis.

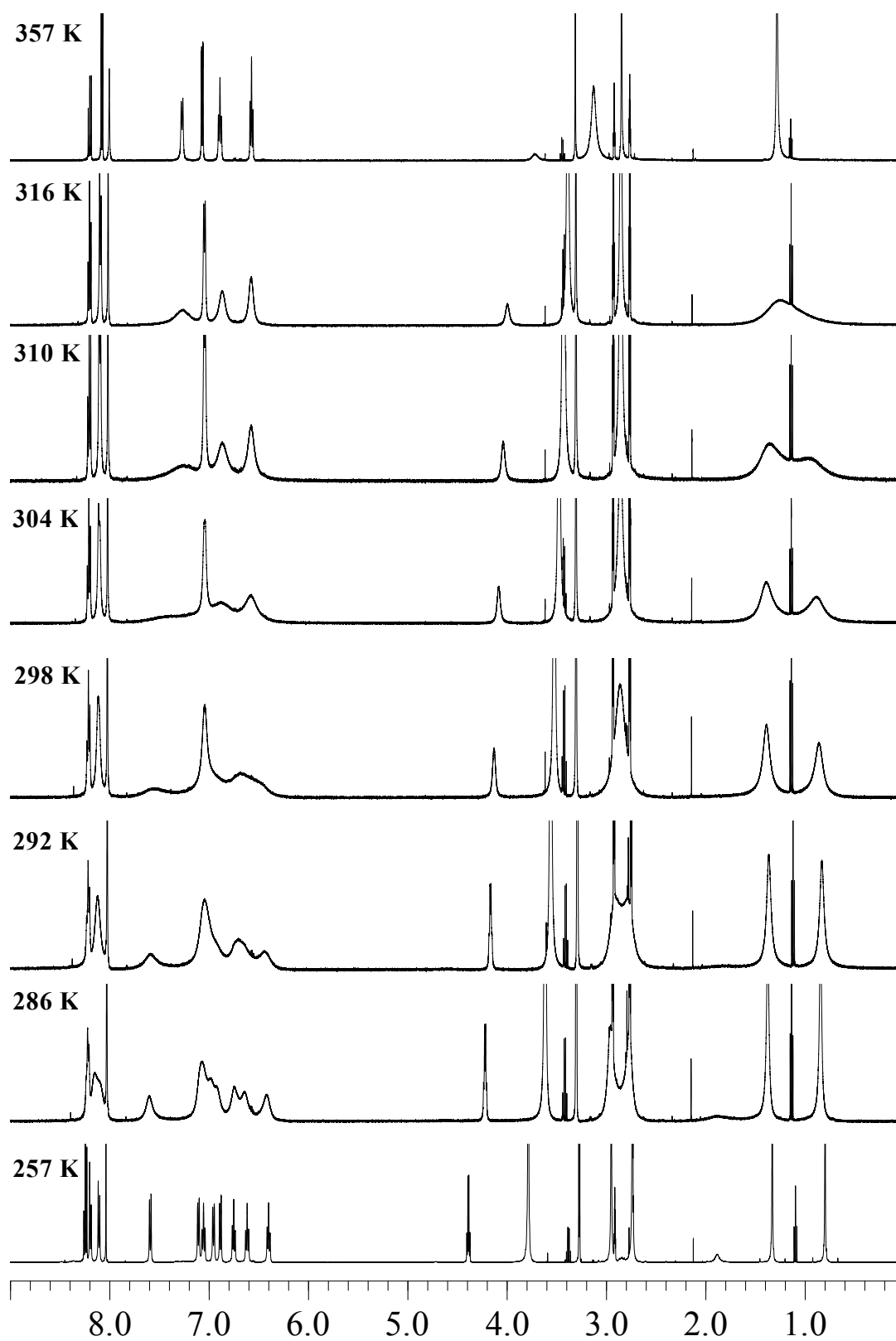


Figure 9. Selected Variable-Temperature ¹H NMR spectra of [Zn₄(L)₂(O₂CCH₃)₄] (**1a**) in the range of 257 to 357 K. The assignment of the peaks is given in the main text of the article.

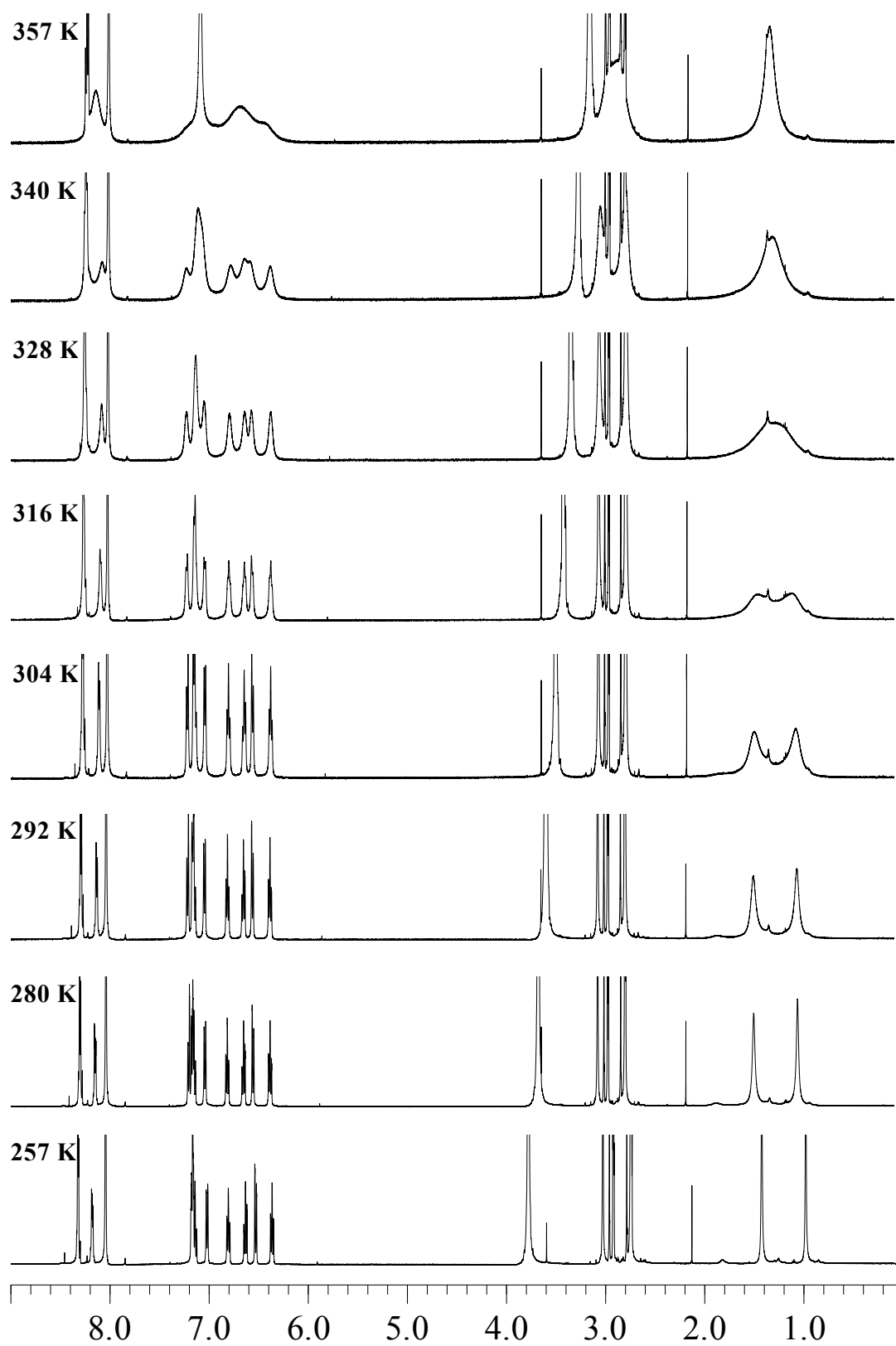


Figure 10. Selected Variable-Temperature ^1H NMR spectra of $[\text{Cd}_4(\text{L})_2(\text{O}_2\text{CCH}_3)_4]$ (**2a**) in the range of 257 to 357 K. The assignment of the peaks is given in the main text of the article.

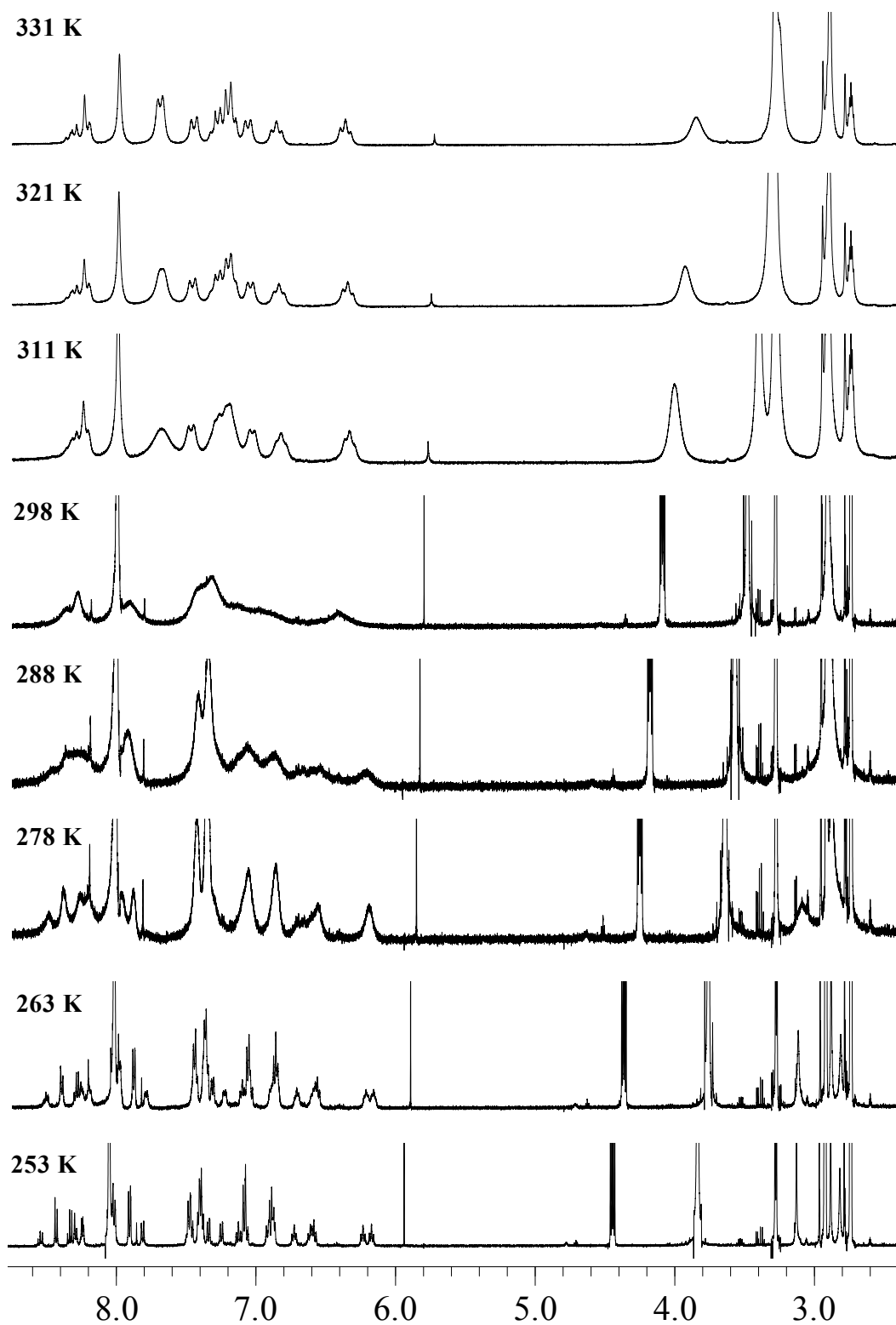


Figure 11. Selected Variable-Temperature ¹H NMR spectra of [Zn₄(L)₂(O₂CC₆H₅)₄] (**1b**) in the range of 253 to 331 K. The spectra at 311, 321 and 331 K were measured on a 200 MHz, the other spectra on a 500 MHz. The assignment of the peaks is given in the main text of the article.

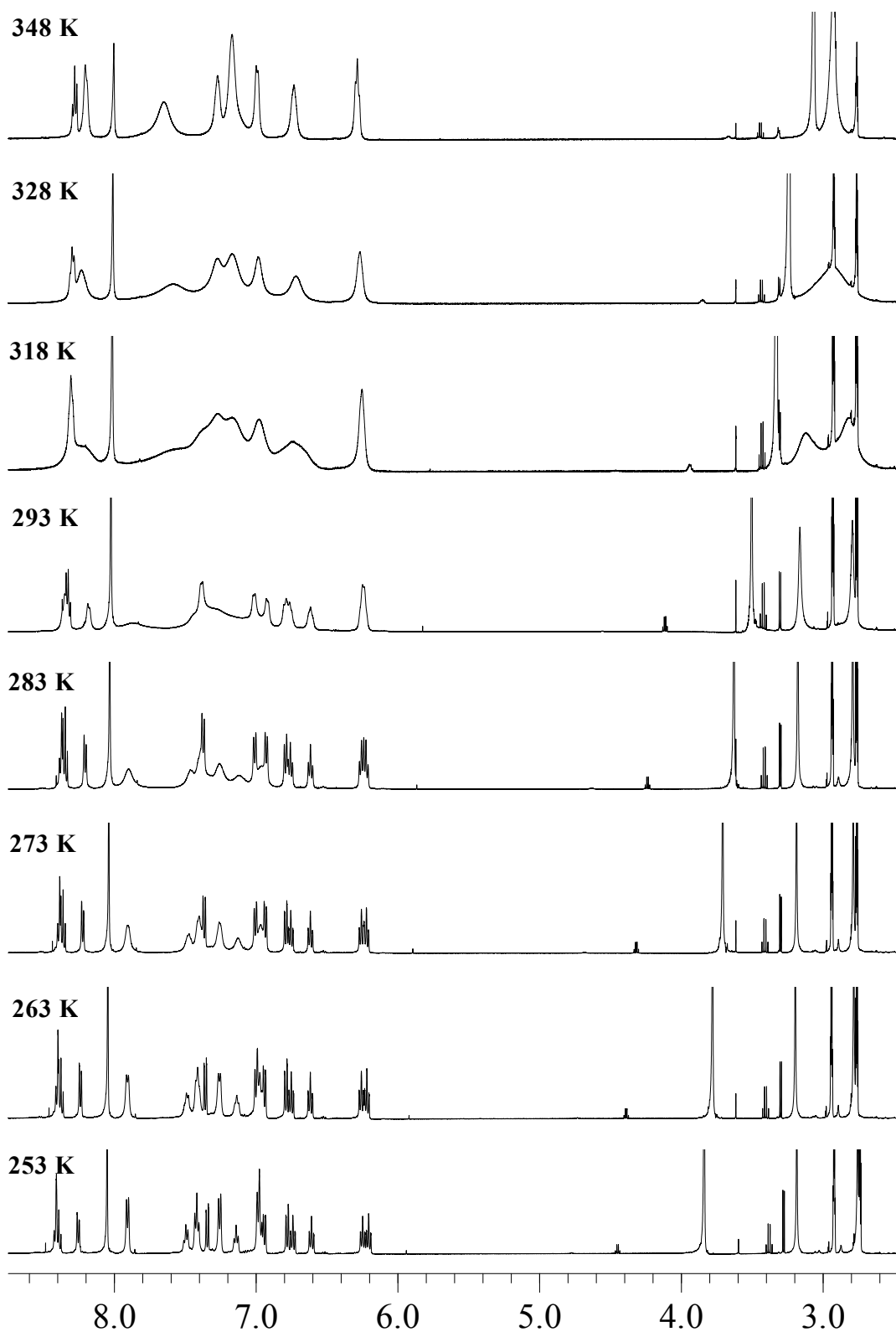


Figure 12. Selected Variable-Temperature ¹H NMR spectra of [Cd₄(L)₂(O₂CC₆H₅)₄] (**2b**) in the range of 253 to 348 K. The assignment of the peaks is given in the main text of the article.

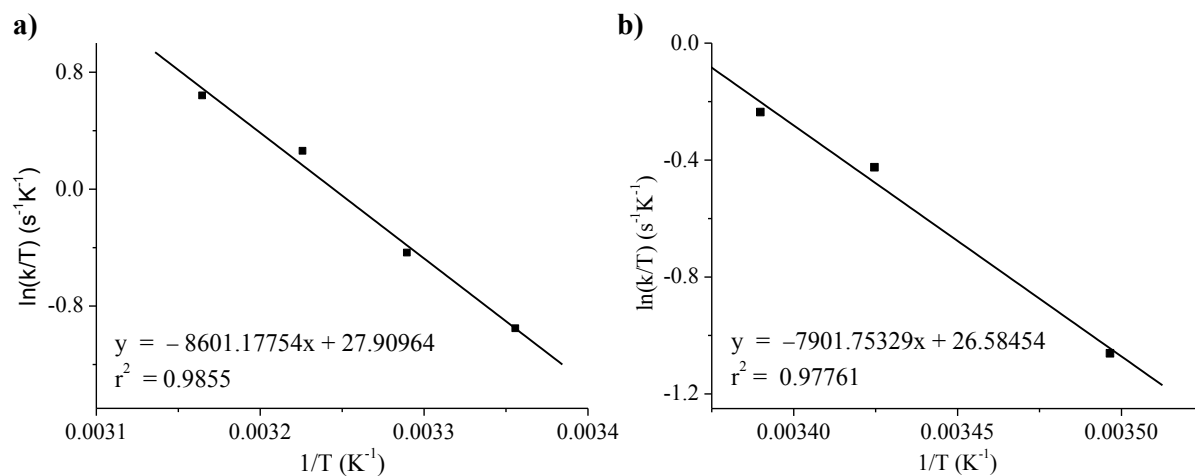


Figure 13. Eyring plot of dynamics for $[Zn_4(L)_2(O_2CCH_3)_4]$ (**1a**) calculated from VT 1H NMR spectra. a) Plot of the protons 8 and 9, which are the acetate ligands. b) Plot of the protons 3, which are the methyl groups on the imine.

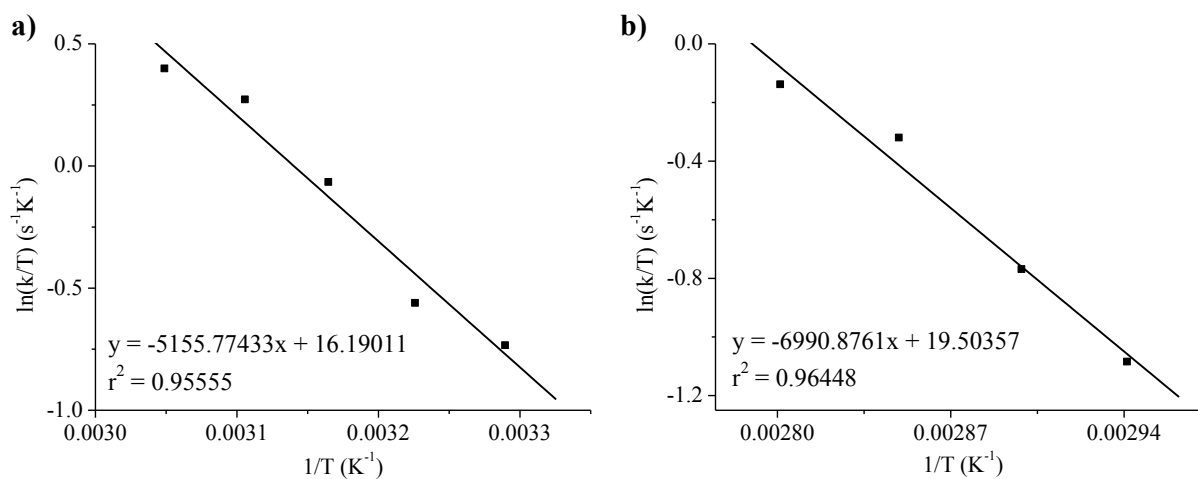


Figure 14. Eyring plots of dynamics for $[Cd_4(L)_2(O_2CCH_3)_4]$ (**2a**) calculated from VT 1H NMR spectra. a) Plot of the protons 8 and 9, which are the acetate ligands. b) Plot of the protons 3, which are the methyl groups on the imine.

References

- (1) Alcock, N. W.; Kingston, R. G.; Moore, P.; Pierpoint, C. *J. Chem. Soc., Dalton Trans.*, **1984**, 1937-1943
- (2) Spectral Database for Organic Compounds (SDBS), **2010**, <http://www.aist.go.jp/>.
- (3) Egashira, T.; Sakai, K.; Takayama, F.; Sakurai, M.; Yoshida, S. *Toxicol. Lett.*, **2003**, *145*, 161.
- (4) Liles, D. C.; Mcpartlin, M.; Tasker, P. A.; Lip, H. C.; Lindloy, L. F. *J. Chem. Soc., Chem. Commun.* **1976**, *14*, 549.
- (5) Sheldrick, G. M. *University of Göttingen, Germany*, **1996**.
- (6) Beurskens, P. T.; Beurskens, G.; Bosman, W. P.; de Gelder, R.; Garcia-Granda, S.; Gould, R.O.; Israel, R.; Smits, J. M. M. *University of Nijmegen, The Netherlands*, **1996**.
- (7) Sheldrick, G. M. *University of Göttingen, Germany*, **1997**.
- (8) (a) Kogler, F. R.; Jupa, M.; Puchberger, M.; Schubert, U. *J. Mater. Chem.* **2004**, *14*, 3133. (b) Puchberger, M.; Kogler, F. R.; Jupa, M.; Gross, S.; Fric, H.; Kickelbick, G.; Schubert, U. *Eur. J. Inorg. Chem.* **2006**, *16*, 3283. (c) Walther, P.; Puchberger, M.; Kogler, F. R.; Schwarz, K.; Schubert, U. *Phys. Chem. Chem. Phys.* **2009**, *11*, 3640. (d) Ye, B.-Y.; Li, X.-Y.; Williams, I. D.; Chen, X.-M. *Inorg. Chem.* **2002**, *41*, 6426.
- (9) (a) Piszczek, P.; Richert, M.; Grodzicki, A.; Glowiak, T.; Wojtczak, A. *Polyhedron* **2005**, *24*, 663. (b) Piszczek, P.; Richert, M.; Wojtczak, A. *Polyhedron* **2008**, *27*, 602.
- (10) (a) Britovsek, G. J. P.; Bruce, M.; Gibson, V. C.; Kimberley, B. S.; Maddox, P. J.; Mastroianni, S.; McTavish, S. J.; Redshaw, C.; Solan, G. A.; Stroemberg, S.; White, A. J. P.; Williams, D. J. *J. Am. Chem. Soc.* **1999**, *121*, 8728. (b) Sugiyama, H.; Korobkov, I.; Gambarotta, S.; Moeller, A.; Budzelaar, P. H. M. *Inorg Chem.* **2004**, *43*, 5771.
- (11) *VT-Calibration manual*; Bruker Instruments, Inc.
- (12) Pons, M.; Millet, O. *Prog. Nucl. Magn. Reson. Spectrosc.* **2001**, *38*, 267.
- (13) Sandström, J. *Dynamic NMR Spectroscopy*; Academic Press: London, **1982**.
- (14) Sutherland, I. O. *Ann. Rep. NMR Spectrosc.* **1971**, *4*, 71.
- (15) Raban, M.; Kost, D.; Carlson, E. H. *J. Chem. Soc., Chem. Commun.* **1971**, *13*, 656.